Hindawi
Shock and Vibration
Volume 2019, Article ID 4937595, 9 pages
https://doi.org/10.1155/2019/4937595

Research Article

An EEMD-Based Denoising Method for Seismic Signal of High Arch Dam Combining Wavelet with Singular Spectrum Analysis

Bo Li,[1] **Lixin Zhang**,[2,3] **Qiling Zhang**,[1] **and Shengmei Yang**[1]

[1]*Engineering Safety and Disaster Prevention Department, Changjiang River Scientific Research Institute, Wuhan, Hubei, China*
[2]*College of Civil Engineering, North Minzu University, Yinchuan, Ningxia, China*
[3]*School of Civil Engineering, Qinghai Nationalities University, Xining, Qinghai, China*

Correspondence should be addressed to Lixin Zhang; zhanglixin2004@163.com

Received 25 October 2018; Revised 14 December 2018; Accepted 25 December 2018; Published 10 March 2019

Academic Editor: José J. Rangel-Magdaleno

Due to complicated noise interference, seismic signals of high arch dam are of nonstationarity and a low signal-to-noise ratio (SNR) during acquisition process. The traditional denoising method may have filtered effective seismic signals of high arch dams. A self-adaptive denoising method based on ensemble empirical mode decomposition (EEMD) combining wavelet threshold with singular spectrum analysis (SSA) is proposed in this paper. Based on the EEMD result for seismic signals of high arch dams, a continuous mean square error criterion is used to distinguish high-frequency and low-frequency components of the intrinsic mode functions (IMFs). Denoised high-frequency IMF using wavelet threshold is reconstructed with low-frequency components, and SSA is implemented for the reconstructed signal. Simulation signal denoising analysis indicates that the proposed method can significantly reduce mean square error under low SNR condition, and the overall denoising effect is superior to EEMD and EEMD-Wavelet threshold denoising algorithms. Denoising analysis of measured seismic signals of high arch dams shows that the performance of denoised seismic signals using EEMD-Wavelet-SSA is obviously improved, and natural frequencies of the high arch dams can be effectively identified.

1. Introduction

Affected by the testing system and environmental factors, seismic signals of high arch dams are unavoidably interfered by complicated noises during the acquisition process, which greatly influences identification and analysis of real signal information. Moreover, chaotic and complicated dynamic behaviors of seismic signals of high arch dams always result in full or partial overlapping of frequency bands of real signals and superimposed noise. It is difficult for the traditional linear method to realize effective denoising. How to remove the noise in seismic signals of high arch dams and improve the reliability and accuracy of test data constitute the foundation for analytical investigations on seismic signals of high arch dams. Some scholars have carried out a large quantity of studies on vibration signal denoising methods [1], where wavelet analysis is a mature signal analysis method with favorable local time-frequency analysis performance. Donoho [2] proposed a threshold denoising method based on wavelet analysis, and this method can obtain optimal estimated value in the Besov space. Therefore, it has been widely applied in signal denoising field [3, 4]. Basic contracting functions of this method include soft threshold function and hard threshold function, both of which have achieved good effect in signal denoising field, but they still have certain deficiencies in aspects of the continuity and approximation to the original signal. Due to complicated service environment and a low signal-to-noise ratio (SNR), denoising effect using wavelet is not ideal [5]. Huang et al. [6] put forward a new signal processing method, namely, empirical mode decomposition (EMD) algorithm. As a self-adaptive time-frequency analysis method, EMD does not need a priori knowledge of the signal compared with the wavelet transform method, and its decomposition completely depends on the signal itself, so it has favorable time-frequency resolution and has been extensively applied to signal denoising [7, 8] and analysis [9, 10]. However, EMD has deficiencies such as mode mixing [11, 12] and end

effect [13]. Influenced by strong noise, intrinsic mode function (IMF) components decomposed out by EMD will lead to signal distortion. In order to overcome the mode mixing phenomenon in EMD, Wu and Huang [14] put forward ensemble empirical mode decomposition (EEMD) which added white noise in the original signal according to uniform distribution feature of white noise power spectral density so that the signal was continuous in different scales. EEMD reserves EMD advantage in processing nonstationary signals; moreover, it can effectively overcome the mode mixing problem of EMD [15, 16]. However, pure EEMD denoising will suppress effective high-frequency information while removing the high-frequency noise [17, 18]. Some scholars have put forward using the wavelet threshold method to remove high-frequency noises in EEMD and reconstructing residual components [19, 20]. However, the wavelet threshold method cannot completely remove high-frequency noises; furthermore, low-frequency IMF is of complicated composition as it is adulterated with low-frequency interharmonics which change with structural operation conditions. Broomhead and King [21] put forward a singular spectrum analysis (SSA) method which was based on singular value decomposition and could decompose the original signal into a series of independent and explainable principal components [22]. The SSA can be an effective and powerful tool to decompose the signal into a set of additive time series from which identifying the interest signal from noise is carried out [23]. Full advantages of EEMD, wavelet threshold denoising method, and SSA are taken in this paper. Wavelet threshold denoising is carried out for high-frequency IMFs with many noises discarded by EEMD in order to reserve effective information in these components. The SSA is implemented for the reconstructed signal. Denoising results of simulation signal and seismic signal of high arch dam are realized. Comparative analyses of the denoising method proposed in this paper with EEMD and EEMD-Wavelet are conducted. Results show that this method is better than EEMD and EEMD-Wavelet on the whole.

The rest of this paper is structured as follows. Sections 2 describes EEMD, Wavelet, and SSA methods, respectively. Section 3 presents the EEMD-Wavelet-SSA denoising method for noise signal. Section 4 demonstrates a simulation signal analysis case to measure the performance of the proposed EEMD-Wavelet-SSA method. Section 5 compares the EEMD-wavelet-SSA method with EEMD and EEMD-Wavelet methods with the use of a seismic signal of high arch dam. Lastly, Section 6 provides the conclusions drawn in this paper.

2. Denoising Method

2.1. Ensemble Empirical Mode Decomposition Method. The EEMD is a new EMD-based signal processing method to solve easy mode mixing effect of EMD. This method makes the signal be of continuity at different scales by virtue of uniform distribution feature of the Gaussian white noise frequency. The noises are offset by multiple averaging processing so as to inhibit and even completely eliminate noise influence [24]. The procedures for implementing EEMD are as follows:

(1) The Gaussian white noise is added to the original signal, whose mean value is 0 and amplitude and standard deviation are constants. The noised signal is shown as

$$x_i(t) = x(t) + n_i(t), \tag{1}$$

where $x_i(t)$ is the signal added with the Gaussian white noise, $n_i(t)$ is the Gaussian white noise, $i = 1, 2, \ldots, M$, and M is the superposition time.

(2) EMD of $x_i(t)$ is implemented to obtain IMFs $c_{ij}(t)$ and the residual component $r_i(t)$, $j = 1, 2, \ldots, N$.

(3) As the mean value of uncorrelated random sequences is 0, the IMFs obtained through the above steps are put under average operation in order to eliminate the influence of multiple superposition of the Gaussian white noises on real IMF, and the IMF after averaging is obtained as follows:

$$c_j(t) = \frac{1}{M}\sum_{i=1}^{M} c_{ij}(t), \tag{2}$$

where $c_j(t)$ is the jth IMF component obtained through EEMD of the original signal.

The EEMD result is as follows:

$$x(t) = \sum_{j=1}^{N} c_j(t) + r(t), \tag{3}$$

where $c_j(t)$ indicates various IMF and $r(t)$ is the final residual component.

In terms of the EEMD method, low-frequency IMF component is dominated by a real signal, and the noise is mainly included in high-frequency IMF. The EEMD denoising method refers to discarding one or multiple high-frequency IMFs while reserving low-frequency IMFs. The consecutive mean square error (CMSE) is used in this paper to determine demarcation point between high-frequency and low-frequency IMFs:

$$\begin{aligned}\mathrm{CMSE}(x_k, x_{k+1}) &= \frac{1}{n}\sum_{i=1}^{n}\left[x_k(t_i) - x_{k+1}(t_i)\right]^2 \\ &= \frac{1}{n}\sum_{i=1}^{n}\left[\mathrm{IMF}_k(t_i)\right]^2,\end{aligned} \tag{4}$$

where n is the signal length, N is the number of IMFs, and $\mathrm{IMF}_k(t_i)$ is the reconstruction error of the IMF, $k = 1, 2, \ldots, N-1$.

Based on this criterion, the demarcation point of the signal energy can be determined as follows:

$$j_s = \arg\min\left[\mathrm{CMSE}\left(\widehat{x}_k, \widehat{x}_{k+1}\right)\right], \tag{5}$$

where arg min indicates the function with minimum reconstruction error, $1 \le k \le N-1$.

2.2. Wavelet Threshold Denoising Method. The Wavelet threshold denoising method firstly transforms the signal into the wavelet domain where threshold processing is

implemented to suppress the wavelet coefficient containing random noises. Finally, a denoised signal is obtained by reconstructing the wavelet coefficient. The threshold processing method includes hard threshold value and soft threshold method. The former keeps the wavelet coefficient higher than the threshold unchanged and conducts zero setting of the wavelet coefficients lower than the threshold in subspaces. The latter conducts zeroing contraction of the wavelet coefficient according to one fixed amount, and the new wavelet coefficient is reconstructed to obtain the signal after denoising. The hard threshold method is simple to use, but the overall function is discontinuous, which will lead to additional vibration phenomenon of the reconstructed signal. Although the soft threshold method is continuous as a whole, the wavelet with a large amplitude will generate the attenuation phenomenon, which will cause a constant deviation of the processed signal [5, 25]. Given the deficiencies of hard and soft threshold methods, this paper constructs a new threshold function based on the hard and soft threshold functions. The improved threshold function is expressed as

$$s(x,\lambda) = \begin{cases} 0, & |x| < \lambda, \\ \operatorname{sign}(x)\left(|x| - \dfrac{\lambda}{1+\ln(1+1/a)}\right), & |x| \geq \lambda, \end{cases} \tag{6}$$

where λ is the threshold and a is the adjustment coefficient. When a takes a large value, the improved threshold function is inclined to the soft threshold function. As a approaches 0, the improved threshold function is inclined to hard threshold function. Threshold function type can be adjusted by changing a. A compromise between soft threshold function and hard threshold function is obtained to eliminate the constant deviation of soft threshold function as far as possible and ensure the continuity of the threshold function.

2.3. Singular Spectrum Analysis. The core idea of SSA is to decompose a raw original time series into a sum of subseries, identified as either a trend, periodic, or quasi-periodic component or noise. Then it is followed by the reconstruction of the original series [26]. The time sequence $x\{i\}$ can be obtained through signal sampling, $i = 1, 2, \ldots, L$. If the number of embedded dimensions is m and the time delay is τ, according to embedding theorem, it is embedded into $m \times n$ dimension space as follows:

$$\mathbf{X} = [x(k), x(k+\tau), x(k+2\tau), \ldots, x(k+(m-1)\tau)]^T, \tag{7}$$

where $k = 1, 2, \ldots, n$, $n = L - (m-1)\tau$, and the orbit matrix $\mathbf{X} = [X_1, X_2, \ldots, X_n]$ represents n coordinate points in the phase space.

$\mathbf{C}$ is set as $m \times m$ dimension covariance matrix of $\mathbf{X}$, which is shown as

$$\mathbf{C} = \frac{\mathbf{X}\mathbf{X}^T}{n}. \tag{8}$$

Singular value decomposition of covariance matrix $\mathbf{C}$ is implemented to obtain a group of nonnegative singular values e_i, $i = 1, 2, \ldots, m$. They are sorted in a descending order as $e_1 \geq e_2 \geq \cdots \geq e_m \geq 0$ to constitute a singular spectrum, which represents relative relations of different components in aspects of their energy proportions in the whole system. Great singular values are corresponding to the signal components with large energies, and small singular values are corresponding to noise components in the signal, which constitute the "noise platform". The eigenvector E^k corresponding to e_k is called empirical orthogonal function (EOF), and the kth principal component (PC) is defined as orthogonal projection coefficient of the original sequence $x\{i\}$ on E^k:

$$a_i^k = \sum_{j=1}^{m} x_{i+j} E_j^k, \quad 0 \leq i \leq L - m. \tag{9}$$

The time sequence reconstructed through principal components (PC) and empirical orthogonal function (EOF) is as follows:

$$x_{i+j} = \sum_{k=1}^{m} a_i^k E_j^k, \quad 1 \leq j \leq m. \tag{10}$$

The selection of principal components in SSA is a key problem. If there are too few selected principal components, the feature information of some signals will be lost. If too many principal components are selected, they will contain excess noise components. The number of principal components is determined in this paper under great difference existing between singular entropy increments. Singular entropy increment combines the information entropy with singular value decomposition, and its computational formula is given by

$$\begin{aligned} H_i &= -p_i \ln(p_i), \\ p_i &= \frac{e_i}{\sum_{i=1}^{m} e_i}, \end{aligned} \tag{11}$$

where H_i is the singular entropy increment, e_i is the singular value, and $i = 1, 2, \ldots, m$.

3. Combined Denoising Method

The EEMD denoising method refers to discarding one or multiple high-frequency components (noises) while effective information on corresponding components is eliminated to cause serious signal distortion. The wavelet threshold denoising method can eliminate most noises together with the effective signals of small amplitude. The EEMD, wavelet threshold and SSA are combined in this paper. First of all, the signal is decomposed into IMFs with frequencies ranking from high to low through the EEMD method. The wavelet threshold denoising method is conducted only for high-frequency components while low-frequency IMFs remain unchanged. High-frequency and low-frequency components after denoising are reconstructed together with the residual component, and finally the reconstructed signal is put under SSA. Concrete steps of the denoising algorithm proposed in this paper are as follows:

(1) The interfered seismic signal $x(t)$ is decomposed by using EEMD and the modal components $c_j(t)$ are obtained

(2) The value of j_s is determined according to consecutive mean square error criterion

(3) The threshold determination criterion is selected, wavelet threshold denoising is implemented for mode components $c_1(t) \sim c_{j_s}(t)$, and then mode components $\hat{c}_1(t) \sim \hat{c}_{j_s}(t)$ after denoising are obtained

(4) The signal is reconstructed, $\hat{x}(t) = \sum_{j=1}^{j_s} \hat{c}_j(t) + \sum_{j=j_s+1}^{N-1} c_j(t) + r(t)$

(5) The SSA is carried out for the reconstructed signal to obtain the signal after denoising

The flowchart of the proposed EEMD-Wavelet-SSA denoising algorithm is illustrated in Figure 1.

In this paper, the conventional SNR method is used to evaluate the denoising effect of the simulation signal. Because the real signal cannot be obtained, the conventional SNR method cannot evaluate the denoising effect of the seismic signal. The spectral estimation method is a SNR calculation method with very clear physical significance. This method assumes that the seismic signal has a certain frequency band range (dominant frequency); too high and too low frequencies are noise.

The method first calculates the power spectrum density of the whole signal, determines the frequency range of the effective signal by calculating natural frequencies of the arch dam through the finite element model, then calculates the energy of the signal and noise, and finally obtains the SNR. The calculation equation of the SNR is as follows:

$$\mathrm{SNR}_S = \frac{\sum_{f_L}^{f_H} |\mathrm{PSD}(f)|^2}{\sum_0^{f_c} |\mathrm{PSD}(f)|^2 - \sum_{f_L}^{f_H} |\mathrm{PSD}(f)|^2}, \tag{12}$$

where f_L is the lowest frequency of the effective signal, f_H is the highest frequency of the effective signal, f_c is the highest frequency of the whole signal, and $\mathrm{PSD}(f)$ is the power spectral density of the frequency f.

4. Simulation Analysis

In order to evaluate the advantage of EEMD-Wavelet-SSA denoising algorithm proposed in this paper, free attenuation signal $x(t)$ is established, and numerical verification of noise signal $x_n(t)$ is implemented. Original signal time is 10 s, and sampling frequency is 200 Hz. The calculation formula is shown in equation (13). The random Gaussian white noise with a signal-to-noise ratio of 5 dB is added to constitute the noise signal:

$$\begin{aligned} x(t) = {} & \exp(-0.2t) \times \cos(6\pi t + 0.5 \sin(6\pi t)) \\ & + 0.5 \times \sin(20\pi t). \end{aligned} \tag{13}$$

Figure 2 shows original signal $x(t)$ and noise signal $x_n(t)$ added with random Gaussian white noises. It can be seen that the original signal is basically covered by noises. It is very difficult to extract the original signal from the noise signal with low SNR.

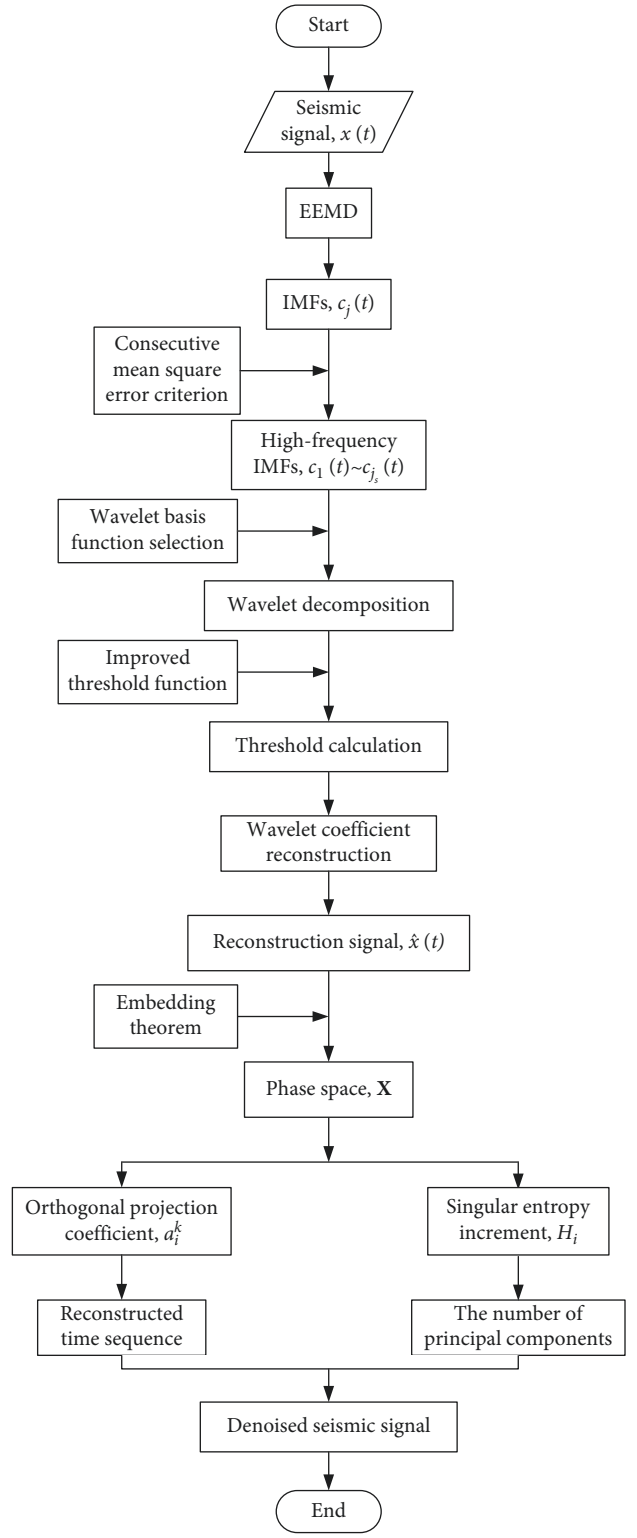

Figure 1: Flowchart of the EEMD-Wavelet-SSA denoising algorithm.

Figure 3 shows EEMD results of the noise signal. The noise signal is decomposed into 9 IMFs and one residual component.

The consecutive mean square error criterion is used to distinguish high-frequency and low-frequency components.

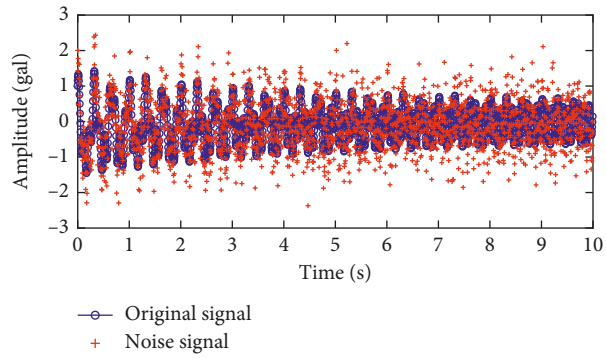

Figure 2: Comparison figure of original signal and noise signal.

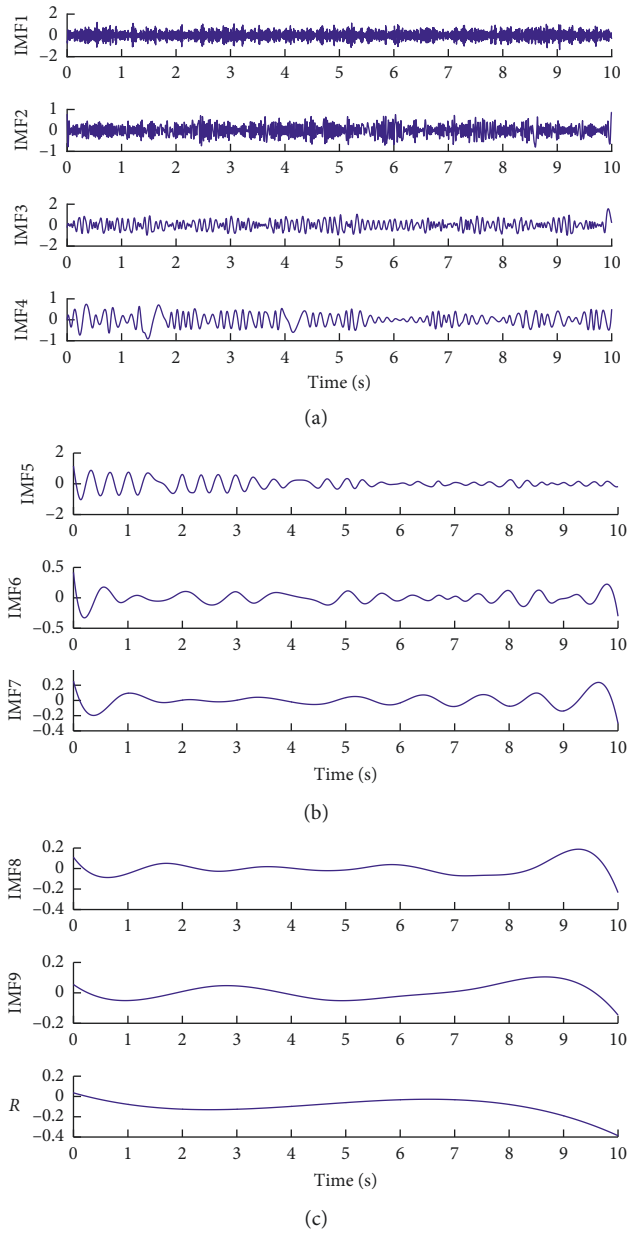

Figure 3: EEMD results of noise signal. (a) IMF1~IMF4. (b) IMF5~IMF7. (c) IMF8, IMF9, and residual component.

According to equations (4) and (5), IMF1~IMF2 are high-frequency signals and IMF3~IMF9 are low-frequency signals. High-frequency components are eliminated while low-frequency components are reserved, and EEMD denoising results are shown in Figure 4. It can be seen that EEMD denoising effect is not ideal, and signal distortion occurs after denoising and some signals appear oscillation.

Wavelet threshold denoising is conducted for high-frequency components of IMF1~IMF2. sym4 wavelet is selected and the number of decomposition layers is 3. High-frequency and low-frequency components after threshold denoising are combined for signal reconstruction. EEMD-Wavelet denoising effect is as shown in Figure 5. The signal waveform is not well recovered after denoising.

The SSA is implemented for the signal after EEMD-Wavelet denoising. Figure 6 shows singular entropy increments of the signal. It can be seen that singular entropy increment of the fifth principal component experiences mutation. The first four principal components are reserved. The final denoising signal is obtained through reconstruction and EEMD-Wavelet-SSA denoising effect is shown in Figure 7. As shown in Figure 7, the signal waveform effect after denoising is superior to EEMD and EEMD-Wavelet denoising effects.

As for the noise signals added with random Gaussian white noises of different SNRs, the calculation results of mean square errors (MSEs) of denoised signals through three methods are shown in Table 1. As can be seen from Table 1, when EEMD is used to remove noise, the denoising signal has the maximum MSE and the minimum SNR, while the EEMD-Wavelet-SSA denoising signal has the minimum MSE and the maximum SNR. The algorithm proposed in this paper is better than EEMD and EEMD-Wavelet on the whole, and its effect on noise signals with low SNRs is more prominent. As the SNR continuously increases, the differences among three methods are narrowed.

5. Engineering Application

A high arch dam is a concrete double-curvature arch dam with a dam height of 285.5 m and design antiseismic intensity is grade 8. The dam body is arranged with 26 monitoring systems for strong motion seismograph (QZY1~QZY26). The site layout of the monitoring systems for strong motion seismograph is shown in Figure 8, and the monitoring system for the strong motion seismograph is shown in Figure 9.

A 3.6 magnitude earthquake occurred nearby this high arch dam on May 8, 2018, and focal depth was 13 km. In order to verify the effectiveness of the method proposed in this paper, measured tangential seismic signal at 527 elevation in 15# dam section is selected as the original signal. The waveform diagram of the original signal is seen, and the gal represents acceleration measurement unit cm/s^2 in Figure 10. As shown in Figure 10, measured signal has strong background noise and it is obviously interfered by noises.

The EEMD of the seismic signal is implemented, and the seismic signal is decomposed into 9 components (IMFl~IMF9) and 1 residual component. Using the

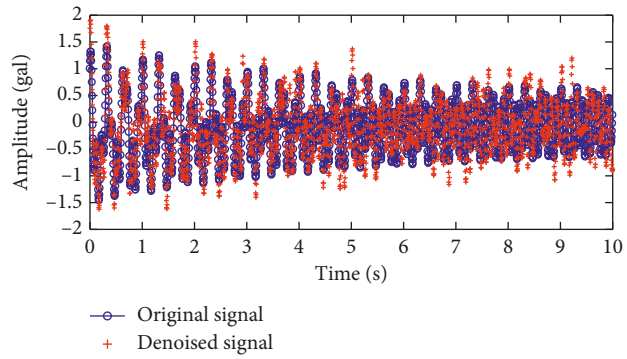

Figure 4: Comparison figure of original signal and denoised signal using EEMD.

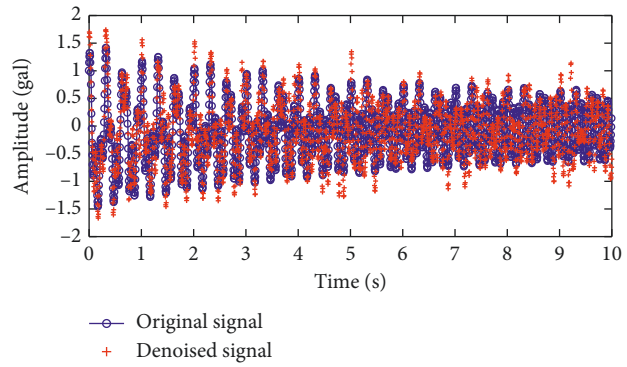

Figure 5: Comparison figure of original signal and denoised signal using EEMD-Wavelet.

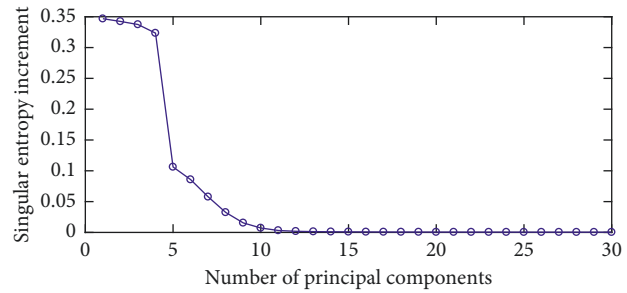

Figure 6: Singular entropy increments of principal components.

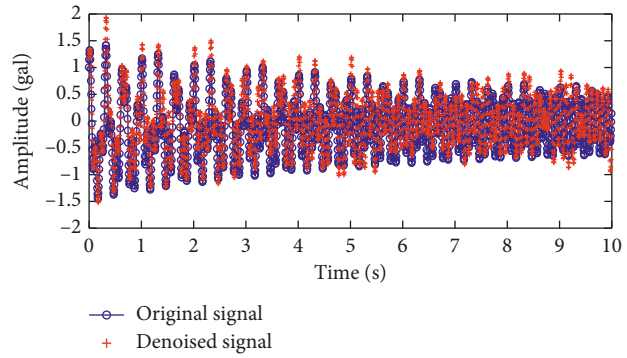

Figure 7: Comparison figure of original signal and denoised signal using EEMD-Wavelet-SSA.

Table 1: Simulation signal denoising effect.

Denoising method	0 dB		5 dB		10 dB	
	MSE	SNR	MSE	SNR	MSE	SNR
EEMD	0.2160	0.8680	0.0730	5.5774	0.0321	9.1420
EEMD-Wavelet	0.1890	1.4472	0.0627	6.2378	0.0230	10.5903
EEMD-Wavelet-SSA	0.1225	3.3301	0.0467	7.5231	0.0229	10.6214

consecutive mean square error criterion, the noises mainly exist in three components (IMFl~IMF3). According to the theorem of the EEMD denoising method, the first 3 high-frequency components are eliminated, and the signal reconstructed is shown in Figure 11. It can be seen from Figure 11 that the signal after denoising is smooth, the noise is effectively eliminated, but the signal amplitude is obviously reduced. The discarded first 3 high-frequency components not only contain the noise but also contain useful information. While eliminating the noise, the EEMD denoising method also eliminates effective information in the first 3 high-frequency components.

The EEMD and wavelet threshold denoising are combined. Three high-frequency components (IMFl~IMF3) are added to the residual components after denoising through wavelet threshold so as to obtain the reconstructed signal. The improved threshold denoising method is adopted during the denoising process. Figure 12 shows denoising results of the seismic signal of the high arch dam combining EEMD with wavelet threshold. As shown in Figure 12, the denoising method combing EEMD with wavelet threshold can basically restore the signal from the noise. The denoising effect is ideal; however, there are some cusps and many burrs in the denoised signal.

Figure 13 shows the denoising result of the seismic signal of the high arch dam combining EEMD, wavelet threshold, and SSA. It can be seen from Figure 13 that the noise is effectively eliminated. The signal after combined denoising is smooth basically without burrs, so the denoising effect is ideal.

In order to compare denoising performances of the three denoising algorithms, the Fourier transform is conducted for the original signal and the signals after EEMD, EEMD-Wavelet, and EEMD-Wavelet-SSA denoising, respectively, to obtain signal spectrum diagrams seen in Figures 14–17. Yin et al. [27] showed the natural frequencies of the first 10 steps of the arch dam are greater than 1 and less than 4. Therefore, it can be judged that the signal with the frequency less than 1 and greater than 4 Hz is noise. From Figures 14–17, it can be seen that

(1) The original signal frequency is distributed on the whole frequency coordinate axis, and power spectrum distribution is obvious in high-frequency components. After EEMD and EEMD-Wavelet-SSA denoising, the power spectrum distribution with frequencies greater than 4 Hz is reduced by a large margin, tending to be 0. The power spectra with frequencies greater than 4 Hz are reduced to a great

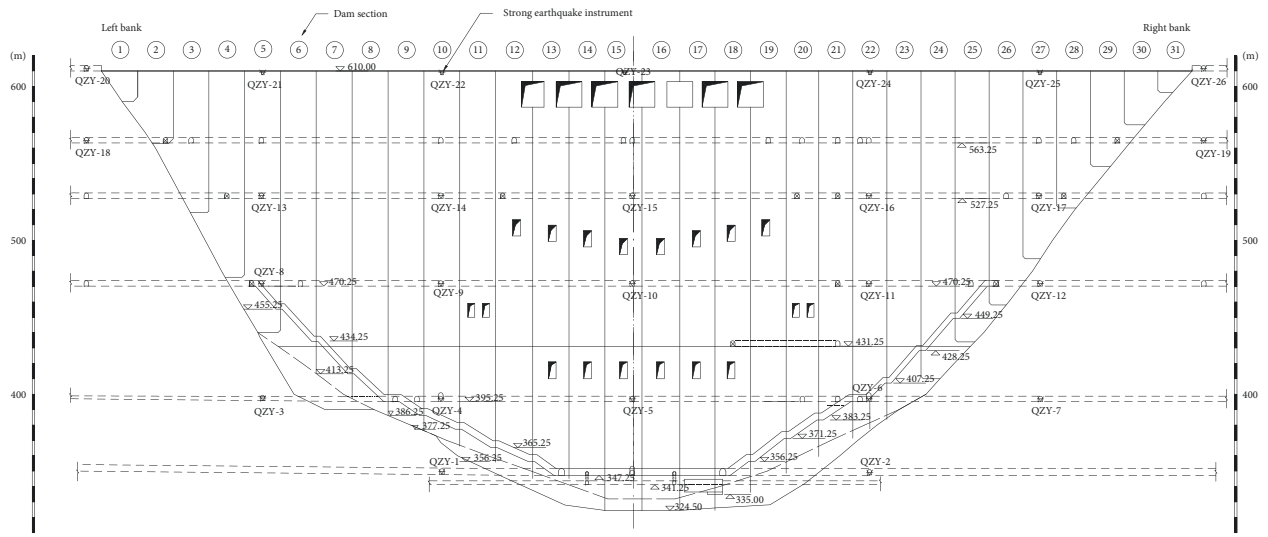

Figure 8: Site layout of the monitoring system for the strong motion seismograph.

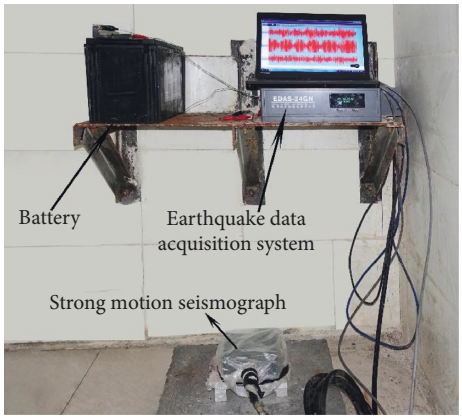

Figure 9: Monitoring system for the strong motion seismograph.

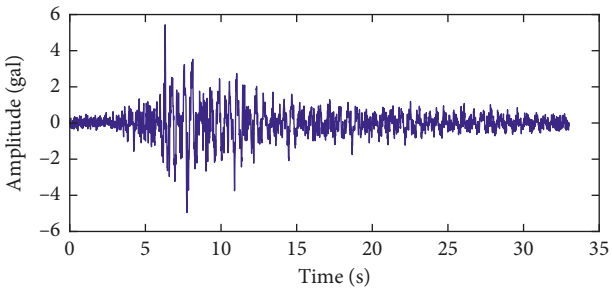

Figure 10: Original signal.

degree but still with a certain distribution after EEMD-Wavelet denoising.

(2) Through a comparison of the spectrum diagrams of the original signal and denoising signal, it could be known that the signal energy after EEMD denoising is obviously reduced, some real signals and noises are eliminated together, which results in signal distortion phenomenon, and only two natural frequencies of the high arch dam could be identified.

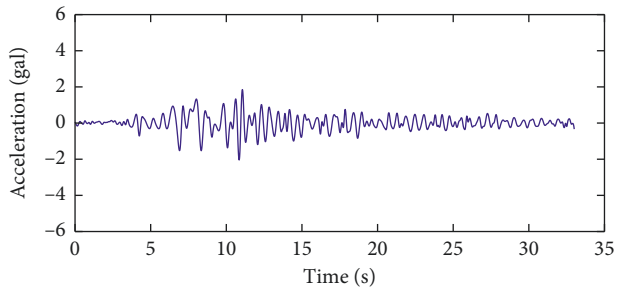

Figure 11: EEMD denoising result.

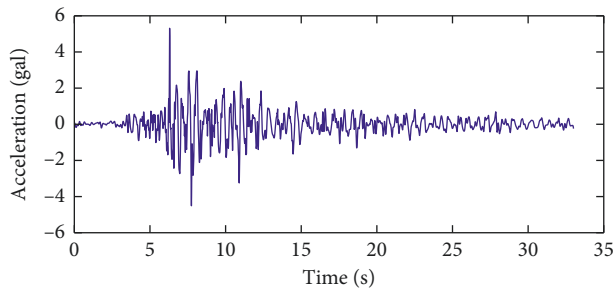

Figure 12: EEMD-Wavelet denoising result.

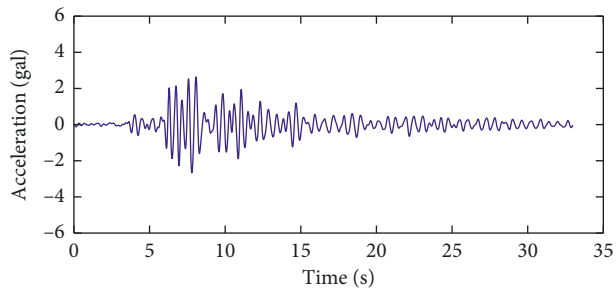

Figure 13: EEMD-Wavelet-SSA denoising result.

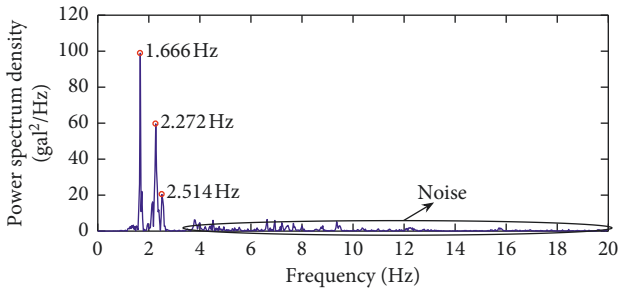

Figure 14: Spectrum diagram of the original signal.

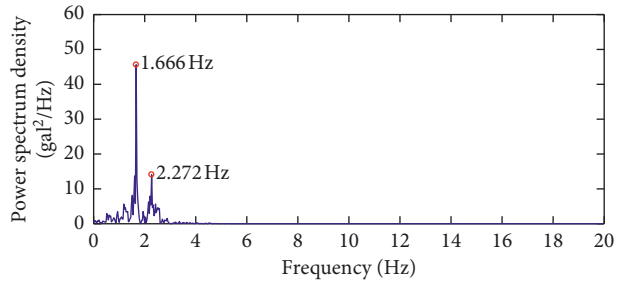

Figure 15: Spectrum diagram of the signal after EEMD denoising.

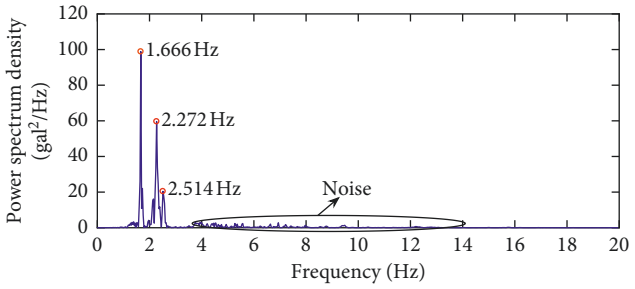

Figure 16: Spectrum diagram of the signal after EEMD-Wavelet denoising.

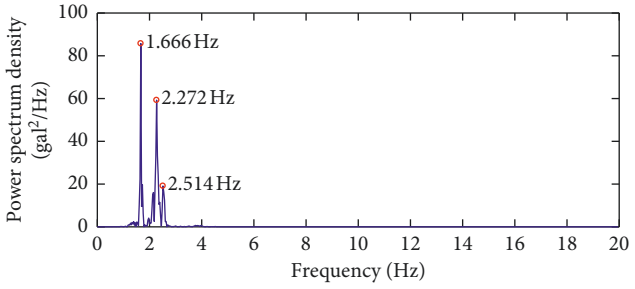

Figure 17: Spectrum diagram of the signal after EEMD-Wavelet-SSA denoising.

Table 2: Seismic signal denoising effect.

Denoising method	SNR
EEMD	51.8016
EEMD-Wavelet	75.8261
EEMD-Wavelet-SSA	5.6335*e*4

EEMD-Wavelet and EEMD-Wavelet-SSA methods effectively extract useful feature information of IMF1~IMF3, avoid signal distortion, and can identify three natural frequencies of the high arch dam.

(3) The spectrum distribution indicates that EEMD and EEMD-Wavelet algorithms have limited denoising ability, and EEMD-Wavelet-SSA algorithm has better denoising effect.

The denoising effect of seismic signal is further analyzed by using the spectral estimation method. According to equation (12) and the natural frequency range of the arch dam, $f_L = 1$, $f_H = 4$, and $f_c = 4$ can be known. The SNR of each denoising method obtained by using equation (12) is shown in Table 2. It can be seen from Table 2 that the SNR of the proposed EEMD-Wavelet-SSA denoising method is the largest, and the denoising effect is obviously better than the other two methods.

6. Conclusions

Given nonstationarity and low SNR features of seismic signals of high arch dams, an EEMD-based signal denoising method combining wavelet threshold and singular spectrum analysis is proposed in this paper. Firstly, the wavelet threshold denoising is conducted for high-frequency IMFs containing many noises which should be discarded by using the EEMD algorithm to reserve effective information of these components. The singular spectrum analysis is used for further denoising of the reconstructed signal so that the signal after denoising reserves waveform features of the original signal very well. The combined denoising method proposed in this paper took full advantages of EEMD, wavelet threshold, and singular spectrum analysis, which can not only effectively remove random noise but also reserve effective information of high-frequency and low-frequency components in the original signal. The simulation signal denoising analysis indicates that the EEMD-Wavelet-SSA denoising method can improve the MSE of the signal with low SNR, which proves that the proposed denoising method can obtain ideal effect.

The denoising analysis of seismic signals of high arch dams shows that the denoising performance of EEMD-Wavelet-SSA is significantly improved compared with the other two methods. Furthermore, this combined method can effectively identify natural frequencies of high arch dam, and it is a satisfactory solution for seismic signal denoising of high arch dam and feature information extraction.

Data Availability

The data used to support the findings of this study are available from the corresponding author upon request.

Conflicts of Interest

The authors declare that they have no conflicts of interest with respect to the research, authorship, and/or publication of this article.

Acknowledgments

This work was supported by the National Natural Science Foundation of China (Grant nos. 51409018, 51579018, and 51509007), the Ningxia Hui Autonomous Region Key R&D Projects (Grant nos. 2018BDE02049 and 2016KJHM126), and Basic Research Program of Qinghai Province (Grant no. 2019-ZJ-7048).

References

[1] S. Mahmoodi, "Anisotropic diffusion for noise removal of band pass signals," *Signal Processing*, vol. 91, no. 5, pp. 1298–1307, 2011.

[2] D. L. Donoho, "De-noising by soft-thresholding," *IEEE Transactions on Information Theory*, vol. 41, no. 3, pp. 613–627, 1995.

[3] X. Jiang, S. Mahadevan, and H. Adeli, "Bayesian wavelet packet denoising for structural system identification," *Structural Control and Health Monitoring*, vol. 14, no. 2, pp. 333–356, 2007.

[4] H.-Y. Lin, S.-Y. Liang, Y.-L. Ho, Y.-H. Lin, and H.-P. Ma, "Discrete-wavelet-transform-based noise removal and feature extraction for ECG signals," *IRBM*, vol. 35, no. 6, pp. 351–361, 2014.

[5] H. Liu, W. Wang, C. Xiang, L. Han, and H. Nie, "A de-noising method using the improved wavelet threshold function based on noise variance estimation," *Mechanical Systems and Signal Processing*, vol. 99, pp. 30–46, 2018.

[6] N. E. Huang, Z. Shen, S. R. Long et al., "The empirical mode decomposition and the Hilbert spectrum for nonlinear and non-stationary time series analysis," *Proceedings of the Royal Society of London. Series A: Mathematical, Physical and Engineering Sciences*, vol. 454, no. 1971, pp. 903–995, 1998.

[7] A. O. Boudraa, J. C. Cexus, and Z. Saidi, "EMD-based signal noise reduction," *International Journal of Signal Processing*, vol. 1, no. 1, pp. 33–37, 2004.

[8] J. Zhang, Q. Jiang, B. Ma, Y. Zhao, and L. Zhu, "Signal de-noising method for vibration signal of flood discharge structure based on combined wavelet and EMD," *Journal of Vibration and Control*, vol. 23, no. 15, pp. 2401–2417, 2015.

[9] Z. Xu, B. Huang, and F. Zhang, "Improvement of empirical mode decomposition under low sampling rate," *Signal Processing*, vol. 89, no. 11, pp. 2296–2303, 2009.

[10] J. Zheng, J. Cheng, and Y. Yang, "Generalized empirical mode decomposition and its applications to rolling element bearing fault diagnosis," *Mechanical Systems and Signal Processing*, vol. 40, no. 1, pp. 136–153, 2013.

[11] X. Y. Hu, S. L. Peng, and W. L. Hwang, "EMD revisited: a new understanding of the envelope and resolving the mode-mixing problem in AM-FM signals," *IEEE Transactions on Signal Processing*, vol. 60, no. 3, pp. 1075–1086, 2012.

[12] J. Zheng, J. Cheng, and Y. Yang, "Partly ensemble empirical mode decomposition: an improved noise-assisted method for eliminating mode mixing," *Signal Processing*, vol. 96, pp. 362–374, 2014.

[13] Z. He, Y. Shen, and Q. Wang, "Boundary extension for Hilbert-Huang transform inspired by gray prediction model," *Signal Processing*, vol. 92, no. 3, pp. 685–697, 2012.

[14] Z. Wu and N. E. Huang, "Ensemble empirical mode decomposition: a noise-assisted data analysis method," *Advances in Adaptive Data Analysis*, vol. 1, no. 1, pp. 1–41, 2009.

[15] H. Jiang, C. Li, and H. Li, "An improved EEMD with multiwavelet packet for rotating machinery multi-fault diagnosis," *Mechanical Systems and Signal Processing*, vol. 36, no. 2, pp. 225–239, 2013.

[16] X. Xue, J. Zhou, Y. Xu, W. Zhu, and C. Li, "An adaptively fast ensemble empirical mode decomposition method and its applications to rolling element bearing fault diagnosis," *Mechanical Systems and Signal Processing*, vol. 62-63, pp. 444–459, 2015.

[17] J.-R. Yeh, J.-S. Shieh, and N. E. Huang, "Complementary ensemble empirical mode decomposition: a novel noise enhanced data analysis method," *Advances in Adaptive Data Analysis*, vol. 2, no. 2, pp. 135–156, 2010.

[18] T.-Y. Wu, H.-C. Hong, and Y.-L. Chung, "A looseness identification approach for rotating machinery based on post-processing of ensemble empirical mode decomposition and autoregressive modeling," *Journal of Vibration and Control*, vol. 18, no. 6, pp. 796–807, 2012.

[19] Y. Kopsinis and S. McLaughlin, "Development of EMD-based denoising methods inspired by wavelet thresholding," *IEEE Transactions on Signal Processing*, vol. 57, no. 4, pp. 1351–1362, 2009.

[20] Y. Zhang, J. Lian, and F. Liu, "An improved filtering method based on EEMD and wavelet-threshold for modal parameter identification of hydraulic structure," *Mechanical Systems and Signal Processing*, vol. 68-69, pp. 316–329, 2016.

[21] D. S. Broomhead and G. P. King, "On the qualitative analysis of experimental dynamical systems," *Physica D: Nonlinear Phenomena*, vol. 20, no. 2-3, pp. 217–236, 1986.

[22] H. Hassani, "Singular spectrum analysis: methodology and comparison," *Journal of Data Science*, vol. 5, no. 2, pp. 239–257, 2007.

[23] F. Romero, F. J. Alonso, J. Cubero, and G. Galán-Marín, "An automatic SSA-based de-noising and smoothing technique for surface electromyography signals," *Biomedical Signal Processing and Control*, vol. 18, pp. 317–324, 2015.

[24] N.-S. Kim, K. Chung, S. Ahn, J. W. Yu, and K. Choi, "Denoising traffic collision data using ensemble empirical mode decomposition (EEMD) and its application for constructing continuous risk profile (CRP)," *Accident Analysis and Prevention*, vol. 71, pp. 29–37, 2014.

[25] X. Chiementin, B. Kilundu, L. Rasolofondraibe, S. Crequy, and B. Pottier, "Performance of wavelet denoising in vibration analysis: highlighting," *Journal of Vibration and Control*, vol. 18, no. 6, pp. 850–858, 2011.

[26] C. Yu, Y. Li, and M. Zhang, "Comparative study on three new hybrid models using Elman neural network and empirical mode decomposition based technologies improved by singular spectrum analysis for hour-ahead wind speed forecasting," *Energy Conversion and Management*, vol. 147, pp. 75–85, 2017.

[27] X. J. Yin, G. L. Wang, C. H. Zhang, and B. Z. Liao, "Dynamic analysis of Xiluodu arch dam," *Journal of Hydroelectric Engineering*, vol. 23, no. 1, pp. 27–30, 2004.